

We are IntechOpen, the world's leading publisher of Open Access books Built by scientists, for scientists

4,800

Open access books available

122,000

International authors and editors

135M

Downloads

Our authors are among the

154

Countries delivered to

TOP 1%

most cited scientists

12.2%

Contributors from top 500 universities



WEB OF SCIENCE™

Selection of our books indexed in the Book Citation Index
in Web of Science™ Core Collection (BKCI)

Interested in publishing with us?
Contact book.department@intechopen.com

Numbers displayed above are based on latest data collected.
For more information visit www.intechopen.com



Analytical, Numerical and Experimental Studies on Stability of Three-Segment Compression Members with Pinned Ends

Seval Pinarbasi Cuhadaroglu, Erkan Akpınar,
Fuad Okay, Hilal Meydanlı Atalay and Sevket Ozden

Additional information is available at the end of the chapter

<http://dx.doi.org/10.5772/45807>

1. Introduction

In earthquake resistant structural steel design, there are two commonly used structural systems. “Moment resisting frames” consist of beams connected to columns with moment resisting (i.e., rigid) connections. Rigid connection of a steel beam to a steel column requires rigorous connection details. On the other hand, in “braced frames”, the simple (i.e., pinned) connections of beams to columns are allowed since most of the earthquake forces are carried by steel braces connected to joints or frame elements with pinned connections. The load carrying capacity of a braced frame almost entirely based on axial load carrying capacities of the braces. If a brace is under tension in one half-cycle of an earthquake excitation, it will be subjected to compression in the other half cycle. Provided that the connection details are designed properly, the tensile capacity of a brace is usually much higher than its compressive capacity. In fact, the fundamental limit state that governs the behavior of such steel braces under seismic forces is their global buckling behavior under compression.

After detailed evaluation, if a steel braced structure is decided to have insufficient lateral strength/stiffness, it has to be strengthened/stiffened, which can be done by increasing the load carrying capacities of the braces. The key parameter that controls the buckling capacity of a brace is its “slenderness” (Salmon et al., 2009). As the slenderness of a brace decreases, its buckling capacity increases considerably. In order to decrease the slenderness of a brace, either its length has to be decreased, which is usually not possible or practical due to architectural reasons, or its flexural stiffness has to be increased. Flexural stiffness of a brace can be increased by welding steel plates or by wrapping fiber reinforced polymers around the steel section. Analytical studies (e.g., Timoshenko & Gere, 1961) have shown that it

usually leads to more economic designs if only the partial length, instead of the entire length, of the brace is stiffened. This also eliminates possible complications in connection details that have to be considered at the ends of the member.

Nonuniform structural elements are not only used in seismic strengthening and rehabilitation of existing structures. In an attempt to design economic and aesthetic structures, many engineers and architects nowadays prefer to use nonuniform structural elements in their structural designs. However, stability analysis of such nonuniform members is usually much more complex than that of uniform members (e.g., see Li, 2001). In fact, most of the design formulae/charts given in design specifications are developed for uniform members. Thus, there is a need for a practical tool to analyze buckling behavior of nonuniform members.

This study investigates elastic buckling behavior of three-segment symmetric stepped compression members with pinned ends (Fig. 1) using three different approaches: (i) analytical, (ii) numerical and (iii) experimental approaches. As already mentioned, such a member can easily be used to strengthen/rehabilitate an existing steel braced frame or can directly be used in a new construction. Surely, the use of stepped elements is not only limited to the structural engineering applications; they can be used in many other engineering applications, such as in mechanical and aeronautical engineering.

In analytical studies, first the governing equations of the studied stability problem are derived. Then, exact solution to the problem is obtained. Since exact solution requires finding the smallest root of a rather complex characteristic equation which highly depends on initial guess, the governing equation is also solved using a recently developed analytical technique by He (1999), which is called Variational Iteration Method (VIM). Many researchers (e.g., Abulwafa et al., 2007; Batiha et al., 2007; Coskun & Atay, 2007, 2008; Ganji & Sadighi, 2007; Miansari et al., 2008; Ozturk, 2009 and Sweilan & Khader, 2007) have shown that complex engineering problems can easily and successfully be solved using VIM. Recently, VIM has also been applied to stability analysis of compression and flexural members. Coskun and Atay (2009), Atay and Coskun (2009), Okay et al. (2010) and Pinarbasi (2011) have shown that it is much easier to solve the resulting characteristic equation derived using VIM. In this paper, by comparing the approximate VIM results with the exact results, the effectiveness of using VIM in determining buckling loads of multi-segment compression members is investigated.

The problem is also handled, for some special cases, using widely known structural analysis program SAP2000 (CSI, 2008). After determining the buckling load of a uniform member with a hollow rectangular cross section, the stiffness of the member is increased along its length partially in different length ratios and the effect of such stiffening on buckling load of the member is investigated. By comparing numerical results with analytical results, the effectiveness of using such an analysis program in stability analysis of multi-segment elements is also investigated.

Finally, buckling loads of uniform and three-segment stepped steel compression members with hollow rectangular cross section are determined experimentally. In the experiments, the "stiffened" columns are prepared by welding additional steel plates over two sides of the member in such a way that the addition of the plates predominantly increases the

smaller flexural rigidity of the cross section, which governs the buckling behavior of the member. By changing the length of the stiffening plates, i.e., by changing the stiffened length ratio, the degree of overall stiffening is investigated in the experimental study. The experimental study also shows in what extent the *ideal* conditions assumed in analytical and numerical studies can be realized in a laboratory research.

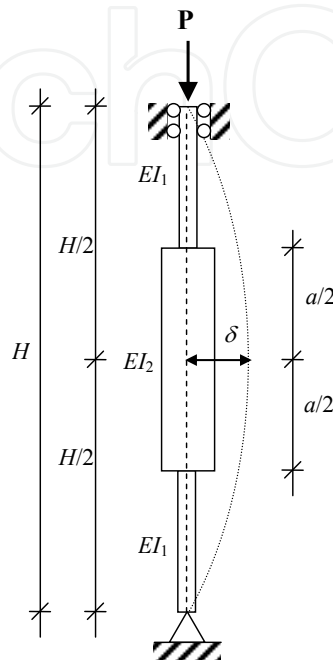


Figure 1. Three-segment symmetric stepped compression member with pinned ends

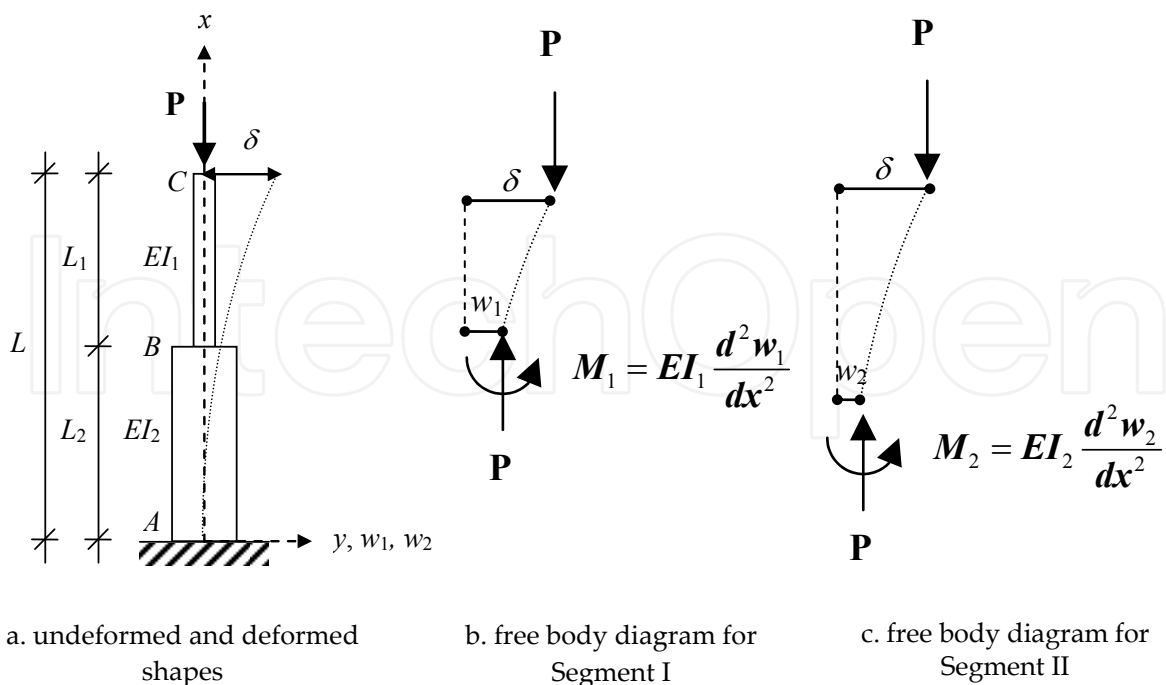


Figure 2. “Equivalent” two-segment stepped compression member with one end fixed (clamped), the other hinged

2. Analytical studies on elastic buckling of a three-segment stepped compression member with pinned ends

2.1. Derivation of governing (buckling) equations

Consider a three-segment symmetric stepped compression member subjected to a compressive load P applied at its top end, as shown in Fig. 1. Assume that both ends of the member are pinned; i.e., free to rotate. Also assume that the top and bottom segments of the member have identical flexural stiffness, EI_1 , while that of the middle segment may be different, say EI_2 . As long as the stiffness variation along the height of the member is symmetric about the mid-height, the buckled shape of the member is also symmetric about the same point as shown in Fig. 1. When such a symmetry exists, the buckling load of the three-segment member can be obtained by analyzing the simpler two-segment member shown in Fig. 2a. This "equivalent" two-segment member has a fixed (clamped) boundary condition at its bottom end whereas its top end is free. From comparison of Fig. 1 and Fig. 2a, one can also see that the length of the equivalent two-segment member equals to the half-length of the original three-segment member, i.e., $L=H/2$. Similarly, $L_2=a/2$. Since the analysis of a two-segment column is much simpler than that of a three-segment column, the analytical study presented in this section is based on the equivalent two-segment member.

The undeformed and deformed shapes of the equivalent two-segment member under uniform compression are illustrated in Fig. 2a. The origin of x - y coordinate system is located at the bottom end of the column. Since the stiffnesses of two segments of the column can be different in general, each segment of the column has to be analyzed separately. Equilibrium equation at an arbitrary section in Segment I can be written from the free body diagram shown in Fig. 2b:

$$EI_1 \frac{d^2 w_1}{dx^2} - P(\delta - w_1) = 0 \quad (1)$$

which can be expressed as

$$\frac{d^2 w_1}{dx^2} + k_1^2 w_1 = k_1^2 \delta \text{ where } k_1^2 = \frac{P}{EI_1} \quad (2)$$

In Eq. (1) and Eq. (2), w_1 is lateral displacement of Segment I at any point, δ is the lateral displacement of the top end of the member, i.e., $\delta = w_1(x=L)$. Eq. (2) is valid for $L_2 \leq x \leq L$. Similarly, from Fig. 2c, the equilibrium equation at an arbitrary section in Segment II can be written as

$$\frac{d^2 w_2}{dx^2} + k_2^2 w_2 = k_2^2 \delta \text{ where } k_2^2 = \frac{P}{EI_2} \quad (3)$$

where w_2 is the displacement of Segment II in y direction. Eq. (3) is valid for $0 \leq x \leq L_2$. For easier computations, the buckling equations in Eq. (2) and Eq. (3) can be written in nondimensional form as follows:

$$(\bar{w}_1)'' + \beta_1^2(\bar{w}_1) = \beta_1^2(\bar{\delta}) \text{ and } (\bar{w}_2)'' + \beta_2^2(\bar{w}_2) = \beta_2^2(\bar{\delta}) \quad (4)$$

with

$$\beta_1 = k_1 L \text{ and } \beta_2 = k_2 L \quad (5)$$

where $\bar{x} = x/L$, $\bar{w}_1 = w_1/L$, $\bar{w}_2 = w_2/L$, $\bar{\delta} = \delta/L$ and prime denotes differentiation with respect to \bar{x} . Since both of the differential equations in Eq. (4) are in second order, the solutions will contain four integration constants. Considering that δ is also unknown, the solution of these buckling equations requires five conditions to determine the resulting five unknowns. Two of these conditions come from the continuity conditions where the flexural stiffness of the column changes and the remaining three conditions are obtained from the boundary conditions at the ends of the column. At $x=L_2$, the lateral displacement and slope functions have to be continuous, which requires

$$[\bar{w}_1]_{\bar{x}=s} = [\bar{w}_2]_{\bar{x}=s} \text{ and } [(\bar{w}_1)']_{\bar{x}=s} = [(\bar{w}_2)']_{\bar{x}=s} \quad (6)$$

where $s = L_2/L$. As far as the boundary conditions are concerned, for a clamped-free column, the end conditions can be written in nondimensional form as:

$$[(\bar{w}_2)]_{\bar{x}=0} = 0, \quad [(\bar{w}_2)']_{\bar{x}=0} = 0 \text{ and } [(\bar{w}_1)]_{\bar{x}=1} = \bar{\delta} \quad (7)$$

Thus, Eq. (4) with Eq. (6) and Eq. (7) constitutes the governing equations for the studied stability problem.

2.2. Exact solution to buckling equations

Since the differential equations given in Eq. (4) are relatively simple, it is not too difficult to obtain their exact solutions, which can be written in the following form:

$$\bar{w}_1 = C_1 \sin(\beta_1 \bar{x}) + C_2 \cos(\beta_1 \bar{x}) + \bar{\delta} \text{ and } \bar{w}_2 = C_3 \sin(\beta_2 \bar{x}) + C_4 \cos(\beta_2 \bar{x}) + \bar{\delta} \quad (8)$$

where C_i ($i=1-4$) are integration constants to be determined from continuity and end conditions. From the first and second conditions given in Eq. (7), one can find that

$$C_3 = 0 \text{ and } C_4 = -\bar{\delta} \quad (9)$$

Then, using Eq. (6), the other integration constants are obtained as:

$$C_1 = \bar{\delta} \left[\frac{\beta_2}{\beta_1} \sin(\beta_2 s) \cos(\beta_1 s) - \cos(\beta_2 s) \sin(\beta_1 s) \right] \quad (10a)$$

$$C_2 = -\bar{\delta} \left[\frac{\beta_2}{\beta_1} \sin(\beta_2 s) \sin(\beta_1 s) + \cos(\beta_2 s) \cos(\beta_1 s) \right] \quad (10b)$$

Finally, the last condition given in Eq. (7) results in

$$\left\{ \tan[\beta_2 s] \tan[\beta_1(1-s)] - \frac{\beta_1}{\beta_2} \right\} \bar{\delta} = 0 \quad (11)$$

For a nontrivial solution, the coefficient term must be equal to zero, yielding the following characteristic equation for the studied buckling problem:

$$\tan[\beta_2 s] \tan[\beta_1(1-s)] = \frac{\beta_1}{\beta_2} \quad (12)$$

Since $\beta_1 / \beta_2 = \sqrt{EI_2 / EI_1}$, if the stiffness ratio n is defined as $n = EI_2 / EI_1$, Eq. (12) can be written in terms of β_1 (square root of nondimensional buckling load of the equivalent two-segment element in terms of EI_1), n (stiffness ratio) and s (stiffened length ratio) as follows:

$$\tan[\beta_1(1-s)] \tan\left[\beta_1 \frac{s}{\sqrt{n}}\right] = \sqrt{n} \quad (13)$$

One can show that the buckling load of the three-segment stepped compression member with length H shown in Fig. 1 can be written in terms of that of the equivalent two-segment member with length $L=H/2$ shown in Fig. 2a as

$$P_{cr} = \lambda \frac{EI_1}{H^2} \text{ where } \lambda = 4\beta_1^2 \quad (14)$$

In other words, λ is the nondimensional buckling load of the three-segment compression member *in terms of* EI_1 .

2.3. VIM solution to buckling equations

According to the variational iteration method (VIM), a general nonlinear differential equation can be written in the following form:

$$Lw(x) + Nw(x) = g(x) \quad (15)$$

where L is a linear operator and N is a nonlinear operator, $g(x)$ is the nonhomogeneous term. Based on VIM, the "correction functional" can be constructed as

$$w_{n+1}(x) = w_n(x) + \int_0^x \lambda(\xi) \{Lw_n(\xi) + N\tilde{w}_n(\xi)\} d\xi \quad (16)$$

where $\lambda(\xi)$ is a general Lagrange multiplier that can be identified optimally via variational theory, w_n is the n -th approximate solution and \tilde{w}_n denotes a restricted variation, i.e., $\delta\tilde{w}_n = 0$ (He, 1999). As summarized in He et al. (2010), for a second order differential equation such as the buckling equations given in Eq. (4), $\lambda(\xi)$ simply equals to

$$\lambda(\xi) = (\xi - x) \tag{17}$$

The original variational iteration algorithm proposed by He (1999) has the following iteration formula:

$$w_{n+1}(x) = w_n(x) + \int_0^x \lambda(\xi) \{Lw_n(\xi) + Nw_n(\xi)\} d\xi \tag{18}$$

In a recent paper, He et al. (2010) proposed two additional variational iteration algorithms for solving various types of differential equations. These algorithms can be expressed as follows:

$$w_{n+1}(x) = w_0(x) + \int_0^x \lambda(\xi) \{Nw_n(\xi)\} d\xi. \tag{19}$$

and

$$w_{n+2}(x) = w_{n+1}(x) + \int_0^x \lambda(\xi) \{Nw_{n+1}(\xi) - Nw_n(\xi)\} d\xi \tag{20}$$

Thus, the three VIM iteration algorithms for the buckling equations given in Eq. (4) can be written as follows:

$$\bar{w}_{i,n+1}(x) = \bar{w}_{i,n}(x) + \int_0^x (\xi - x) \{ \bar{w}_{i,n}''(\xi) + \beta_i^2 \bar{w}_{i,n} - \beta_i^2 \bar{\delta} \} d\xi, \tag{21a}$$

$$\bar{w}_{i,n+1}(x) = \bar{w}_{i,0}(x) + \int_0^x (\xi - x) \{ \beta_i^2 \bar{w}_{i,n} - \beta_i^2 \bar{\delta} \} d\xi, \tag{21b}$$

$$\bar{w}_{i,n+2}(x) = \bar{w}_{i,n+1}(x) + \int_0^x (\xi - x) \{ (\bar{w}_{i,n+1}''(\xi) - \bar{w}_{i,n}''(\xi)) + \beta_i^2 (\bar{w}_{i,n+1} - \bar{w}_{i,n}) \} d\xi, \tag{21c}$$

where i is the segment number and can take the values of one or two. It has already been shown in Pinarbasi (2011) that all VIM algorithms yield exactly the same results for a similar stability problem. For this reason, considering its simplicity, the second iteration algorithm is decided to be used in this study.

Recalling that $\beta_1 / \beta_2 = \sqrt{n}$ and $\lambda = 4\beta_1^2$, the iteration formulas for the buckling equations of the studied problem can be written in terms of λ and n as follows:

$$\bar{w}_{1,j+1}(x) = \bar{w}_{1,0}(x) + \int_0^x (\xi - x) \left\{ \frac{\lambda}{4} (\bar{w}_{1,j} - \bar{\delta}) \right\} d\xi, \tag{22a}$$

$$\bar{w}_{2,j+1}(x) = \bar{w}_{2,0}(x) + \int_0^x (\xi - x) \left\{ \frac{\lambda}{4n} (\bar{w}_{2,j} - \bar{\delta}) \right\} d\xi \tag{22b}$$

As an initial approximation for displacement function of each segment, a linear function with unknown coefficients is used:

$$\bar{w}_{1,0} = C_1 \bar{x} + C_2 \quad \text{and} \quad \bar{w}_{2,0} = C_3 \bar{x} + C_4 \tag{23}$$

where C_i ($i=1-4$) are to be determined from continuity and end conditions. After conducting seventeen iterations, $\bar{w}_{1,17}$ and $\bar{w}_{2,17}$ are obtained. Substituting these approximate solutions to the continuity equations in Eq. (6) and to the end conditions in Eq. (7), five equations are obtained. Four of them are used to determine the unknown coefficients in terms of $\bar{\delta}$, while the remaining one is used to construct the characteristic equation for the studied problem:

$$[F(\lambda)] \bar{\delta} = 0 \tag{24}$$

where $F(\lambda)$ is the coefficient term of $\bar{\delta}$. For a nontrivial solution $F(\lambda)$ must be equal to zero. The smallest possible real root of the characteristic equation gives the nondimensional buckling load ($\lambda = PH^2 / EI_1$) of the three-segment compression member in the first buckling mode.

2.4. Comparison of VIM results with exact results

For various values of stiffness ratio ($n=EI_2/EI_1$) and stiffened length ratio ($s=a/H$), nondimensional buckling loads of a three-segment compression member with pinned ends are determined both by using Eq. (13) and VIM. VIM results are compared with the exact results in Table 1.

n	s							
	0.2		0.4		0.6		0.8	
	Exact	VIM	Exact	VIM	Exact	VIM	Exact	VIM
100	15.344	15.344	27.052	27.052	59.843	59.843	225.706	225.706
10	14.675	14.675	24.006	24.006	44.978	44.978	85.880	85.880
5	13.978	13.978	21.109	21.109	33.471	33.471	46.651	46.651
2.5	12.721	12.721	16.694	16.693	21.275	21.275	24.186	24.186
1.67	11.632	11.632	13.642	13.642	15.406	15.406	16.306	16.306
1.25	10.689	10.689	11.471	11.471	12.039	12.039	12.297	12.297

Table 1. Comparison of VIM predictions for nondimensional buckling load (λ) of a three-segment compression member with exact results for various values of stiffness ratio ($n=EI_2/EI_1$) and stiffened length ratio ($s=a/H$)

As it can be seen from Table 1, VIM results perfectly match with exact results, verifying the efficiency of VIM in this particular stability problem. It is worth noting that it is somewhat difficult to solve the characteristic equation given in Eq. (13) since it is highly sensitive to the initial guess. While solving this equation, one should be aware of that an improper initial guess can result in a buckling load in higher modes. On the other hand, the characteristic equations derived using VIM are composed of polynomials, all roots of which can be obtained more easily. This is one of the strength of VIM even when an exact solution is available for the problem, as in our case.

2.5. VIM results for various stiffness and stiffened length ratios

Table 2 tabulates VIM predictions for nondimensional buckling load of a three-segment stepped compression member for various values of stiffness (n) and stiffened length (s) ratios. The results listed in this table can directly be used by design engineers who design/strengthen three-segment symmetric stepped compression members with pinned ends.

n	s						
	0.1	0.2	0.25	0.3333	0.5	0.75	0.9999
1	9.8696	9.8696	9.8696	9.8696	9.8696	9.8696	9.8696
1.5	10.5592	11.3029	11.6881	12.3342	13.5322	14.6186	14.8044
2	10.9332	12.1571	12.8290	14.0255	16.5379	19.2404	19.7392
2.5	11.1676	12.7211	13.6051	15.2433	19.0149	23.7328	24.6740
3	11.3282	13.1202	14.1651	16.1557	21.0707	28.0942	29.6088
4	11.5338	13.6465	14.9165	17.4239	24.2442	36.4193	39.4784
5	11.6599	13.9775	15.3962	18.2587	26.5469	44.2105	49.3480
7.5	11.8311	14.4372	16.0711	19.4641	30.1728	61.3848	74.0220
10	11.9181	14.6750	16.4240	20.1076	32.2453	75.4700	98.6960
20	12.0504	15.0419	16.9731	21.1249	35.6828	109.4880	197.3920
50	12.1307	15.2680	17.3139	21.7652	37.9220	138.1940	493.4800
100	12.1577	15.3444	17.4295	21.9836	38.6944	148.2010	986.9600

Table 2. VIM predictions for nondimensional buckling load (λ) of a three-segment column for various values of stiffness ratio ($n=EI_2/EI_1$) and stiffened length ratio ($s=a/H$)

At this stage, it can be valuable to investigate the amount of increase in buckling load due to partial stiffening of a compression member. Fig. 3 shows variation of increase in critical buckling load, with respect to the uniform case, with stiffened length ratio for different values of stiffness ratio. From Fig. 3, it can be inferred that there is no need to stiffen entire

length of the member to gain appreciable amount of increase in buckling load especially if n is not too large. For $n=2$, increase in buckling load when only half length of the member is stiffened is more than 80 % of the increase that can be gained when the entire length of the member is stiffened. Fig. 3 also shows that if n increases, to get such an enhancement in buckling load, s has to be increased. For example, when $n=10$, the stiffened length of the member has to be more than 75% of its entire length if similar enhancement in member behavior is required. In fact, this can be seen more easily from Fig. 4 where the increase in buckling load is plotted in terms of stiffness ratio for various stiffened length ratios. Fig. 4 shows that if the stiffened length ratio is small, there is no need to increase the stiffness ratio too much. As an example, if only one-fifth of the entire length of the member is to be stiffened, increase in buckling load when $n=2$ is more than 80% of that when $n=10$. On the other hand, if 75 % of the entire length is allowed to be stiffened, increase in buckling load when $n=2$ is approximately 25% of that when $n=10$.

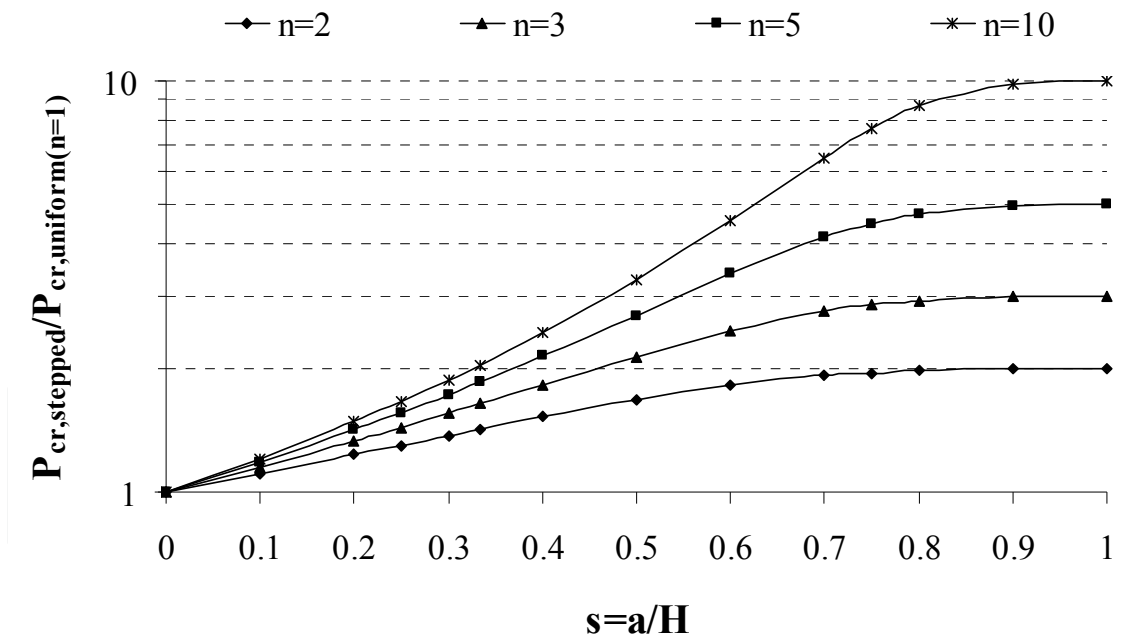


Figure 3. Variation of increase in buckling load with stiffened length ratio (s) for various values of stiffness ratio (n)

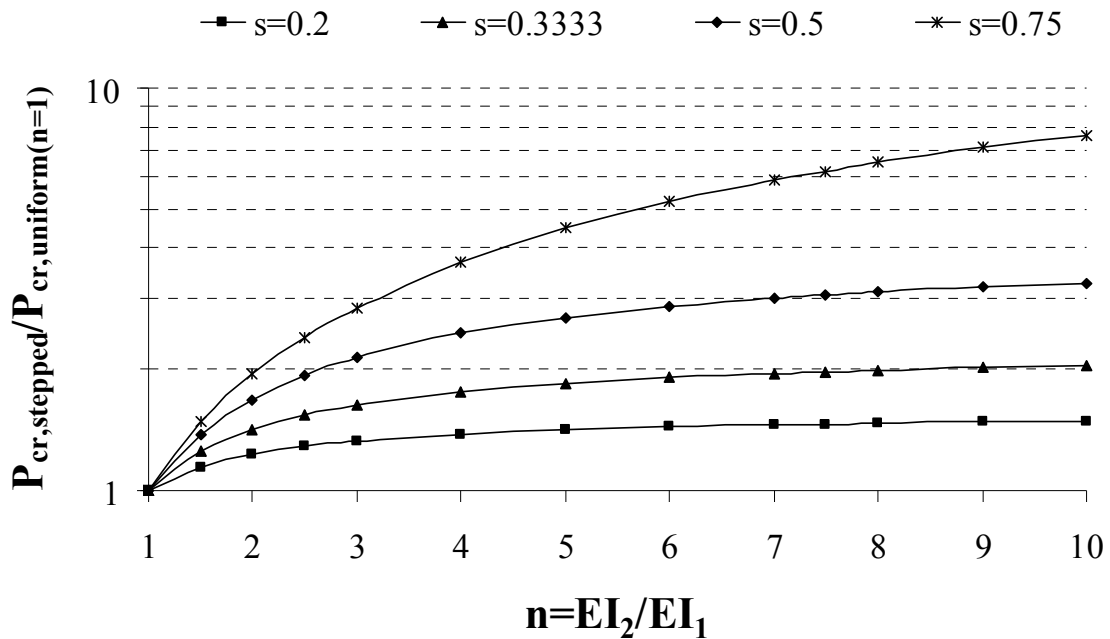
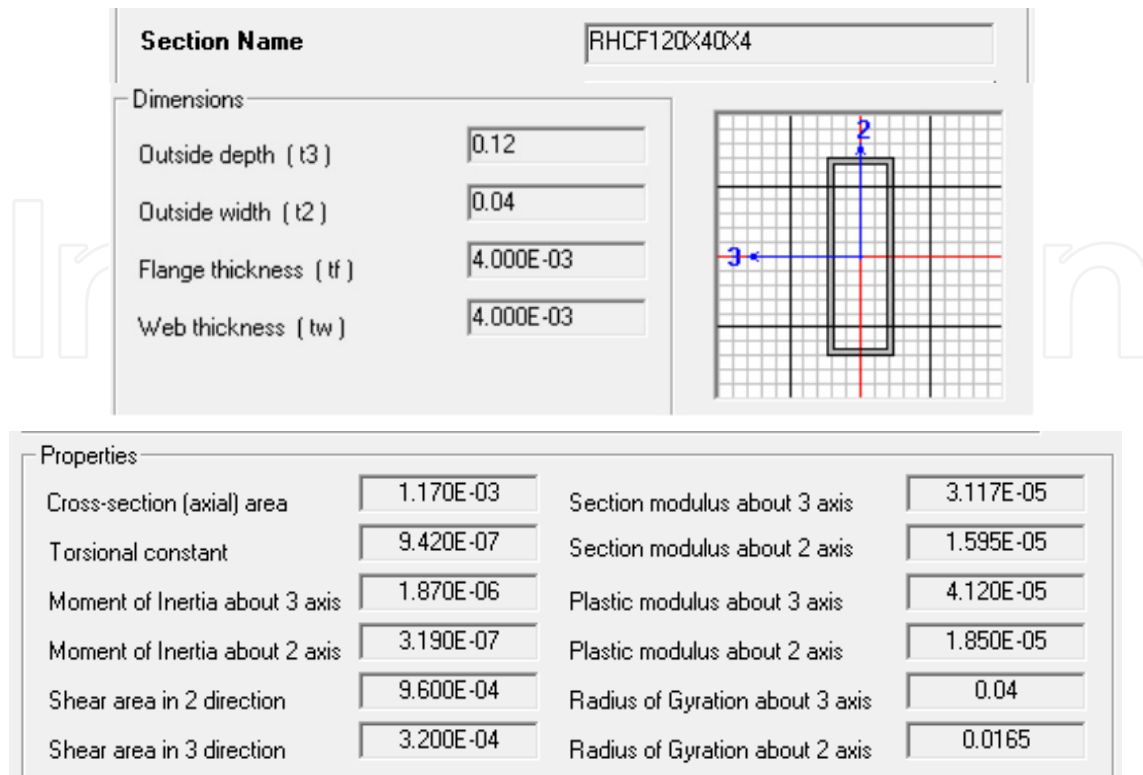


Figure 4. Variation of increase in buckling load with stiffness ratio (n) for various values of stiffened length ratio (s)

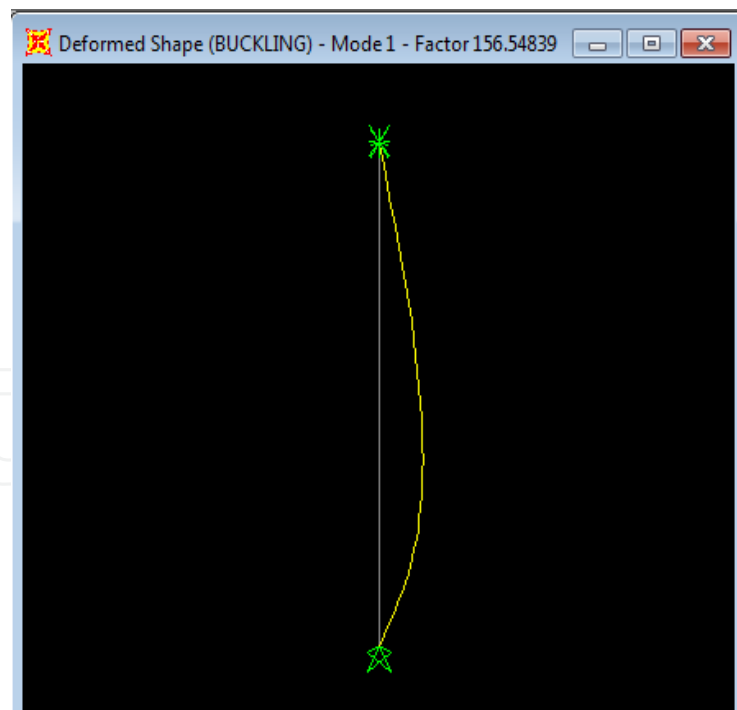
3. Numerical studies on elastic buckling of a three-segment stepped compression member with pinned ends

In order to obtain directly comparable results with the experimental results that will be discussed in the following section, in the numerical analysis, the reference “unstiffened” member is selected to have a hollow rectangular cross section, namely RCF 120x40x4, the geometric properties of which is given in Fig. 5a. The length of the steel (with modulus of elasticity of $E=200$ GPa) columns is chosen to be 2 m., which is the largest height of a compression member that can be tested in the laboratory due to the height limitations of the test setup. Elastic stability (buckling) analysis is performed using a well-known commercial structural analysis program SAP2000 (CSI, 2008).

Fig. 5b shows numerical solutions for the buckled shape and buckling load, $P_{cr,num,n=1} = 156.55$ kN, of the uniform column. Exact value of the buckling load P_{cr} for this column can be computed from the well-known formula of Euler; $P_{cr} = \pi^2 EI / L^2$, which gives $P_{cr,exact,n=1} = 157.42$ kN. The error between the numerical and exact analytical result is only 0.5 %, which encourages the use of this technique in determining the buckling load of “stiffened” members.



a. cross sectional properties (in meters)



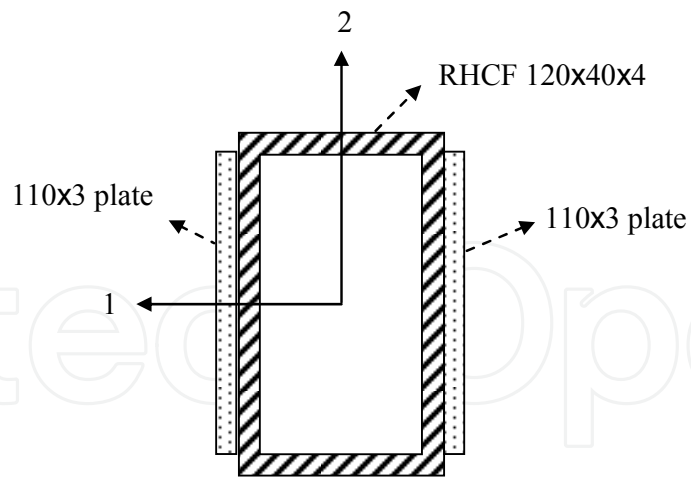
b. buckling load (in kN)

Figure 5. Geometric properties and buckling load of the uniform column ($n=1$) analyzed in numerical study

In the experimental study, in addition to the unstiffened members, three different types of stiffened columns are tested. In these specimens, the stiffness ratio is kept constant ($n \approx 2$) while the stiffened length ratio is varied. The stiffnesses of the three-segment members are increased by welding rectangular steel plates, with 100 mm width and 3 mm thickness as shown in Fig. 6a, to the wider faces of the hollow cross section. The length of the stiffening plates is 0.4 m in members with $s=0.2$, approximately 0.67 m in members with $s=0.3333$ and 1.0 m in members with $s=0.5$. This stiffening method increases the cross sectional area of the section about 1.56 times and major and minor axis flexural rigidities of the cross section, respectively, about 1.36 and 1.96 times. In the numerical analysis, the geometrical properties of the cross section for the stiffened region of the column have to be increased in these ratios. In SAP2000 (CSI, 2008), this step can easily be performed by using “property/stiffness modification factors” command (Fig. 6a). It is to be noted that axis-2 is still the minor axis of the member, so the buckling is expected to be observed about this axis, as in the uniform column case. Fig. 6b shows the buckled shape and buckling load ($P_{cr,num,n=1.96,s=0.2} = 192.30$ kN) of the stiffened members when one-fifth of the entire length of the member is stiffened as illustrated in Fig. 6a; i.e., when $n=1.96$ and $s=0.2$. Similar analyses on members with $s=0.3333$ and $s=0.5$ yield buckling loads of $P_{cr,num,n=1.96,s=0.3333} = 220.42$ kN and $P_{cr,num,n=1.96,s=0.5} = 258.93$ kN, respectively. If these values of buckling loads for stiffened elements are normalized with respect to the buckling load for the uniform member ($P_{cr,num,n=1} = 156.55$ kN), the amount of increase achieved in buckling load in each stiffening scheme is computed approximately as 1.23 when $s=0.2$, 1.41 when $s=0.3333$ and 1.65 when $s=0.5$. To compare numerical results with analytical results, buckling loads for three-segment symmetric stepped columns with $n=1.96$ are determined using VIM for various values of s and increase in buckling load with varying s is plotted in Fig. 7. It can be seen that the approximate results obtained through numerical analysis exactly match with VIM solutions. The effectiveness of the numerical analysis in solving this special buckling problem is examined further for different values of n and s . The results are presented in Table 4, which indicates very good agreement between the analytical and numerical results.

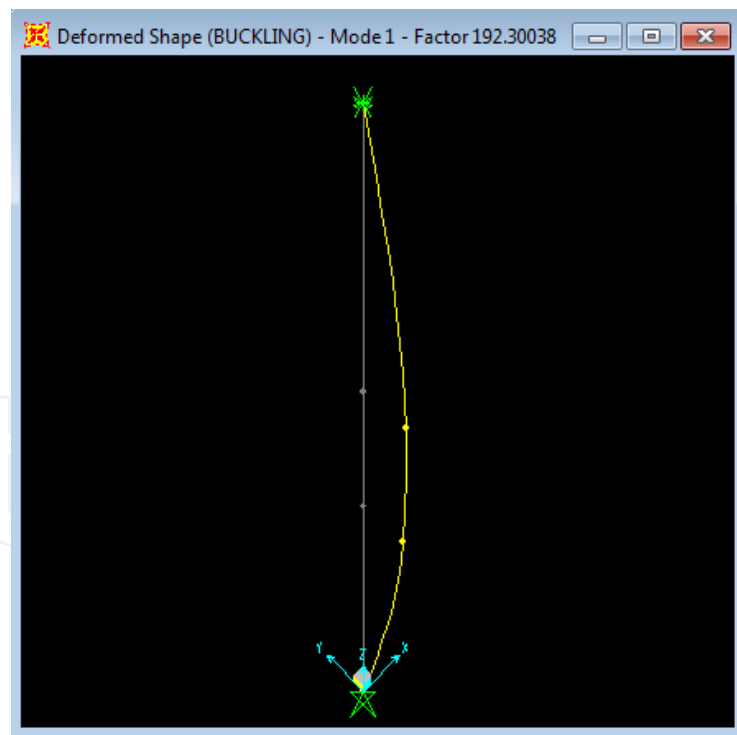
n	s=0.25			s=0.5			s=0.75		
	Exact	VIM	SAP2000	Exact	VIM	SAP2000	Exact	VIM	SAP2000
1.5	1.18	1.18	1.18	1.37	1.37	1.38	1.48	1.48	1.48
2	1.30	1.30	1.30	1.68	1.68	1.68	1.95	1.95	1.93
2.5	1.38	1.38	1.38	1.93	1.93	1.92	2.40	2.40	2.38
3	1.44	1.44	1.44	2.13	2.13	2.13	2.85	2.85	2.80
5	1.56	1.56	1.56	2.69	2.69	2.67	4.48	4.48	4.35
7.5	1.63	1.63	1.63	3.06	3.06	3.03	6.22	6.22	5.94
10	1.66	1.66	1.67	3.27	3.27	3.24	7.65	7.65	7.20

Table 3. Comparison of numerical results with analytical (exact and approximate (VIM)) results for increase in buckling load for a three-segment compression member with pinned ends for various values of stiffness ratio ($n=EI_2/EI_1$) and stiffened length ratio ($s=a/H$)



Property/Stiffness Modifiers for Analysis	
Cross-section (axial) Area	1.5641
Moment of Inertia about 2 axis	1.95793
Moment of Inertia about 3 axis	1.35607

a. area/stiffness modifiers for the stiffened region of the column



b. buckling load (in kN)

Figure 6. Geometric properties and buckling load a three-segment stepped column with stiffened length ratio $s=0.2$ and stiffness ratio $n=1.96$

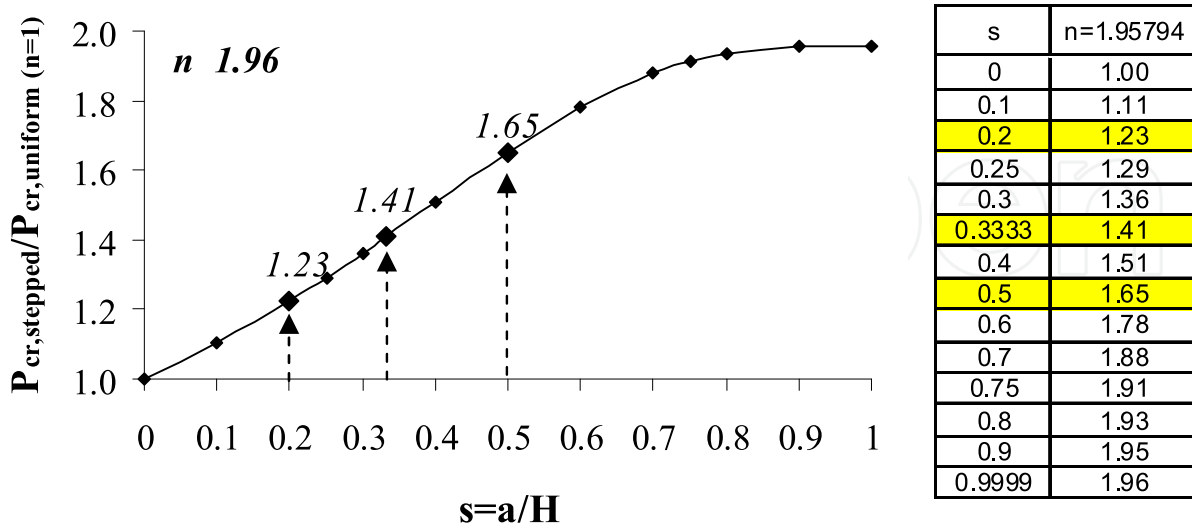


Figure 7. Increase in critical buckling load for various stiffened length ratios (s) when stiffness ratio is $n \cong 1.96$ (VIM results)

4. Experimental studies on elastic buckling of a three-segment stepped compression member with pinned ends

The experimental part of the study is conducted in the Structures Laboratory of Civil Engineering Department in Kocaeli University. Test specimens are subjected to monotonically increasing compressive load until they buckle about their minor axis in a test setup specifically designed for such types of buckling tests (Fig. 8). Due to the height limitations of the test setup, the length of the test specimens is fixed to 2 m. To observe elastic buckling, “unstiffened” (uniform) *reference* specimens are selected to have a rather small cross section; hollow rectangular section with side dimensions of 120 mm x 40 mm and wall thickness of 4 mm, as shown in Fig. 5a. In addition to the three unstiffened specimens, named B0-1, B0-2 and B0-3, three sets of “stiffened” specimens, each of which consists of three columns with identical stiffening, are tested. To obtain comparable results, the stiffness ratio of the stiffened specimens is kept constant ($n \cong 2$) while their stiffened length ratios (s) are varied in each set. Such stiffening is attained by welding rectangular steel plates, with 100 mm width and 3 mm thickness as shown in Fig. 6a, to the wider faces of the hollow cross sections of the test specimens, in different lengths. The length of the stiffening plates is 0.4 m for the members with stiffened length ratio $s=0.2$, which are named B1-1, B1-2 and B1-3, approximately 0.67 m for the members with $s=0.3333$, named B2-1, B2-2 and B2-3, and 1.0 m for the members with $s=0.5$, named B3-1, B3-2 and B3-3.

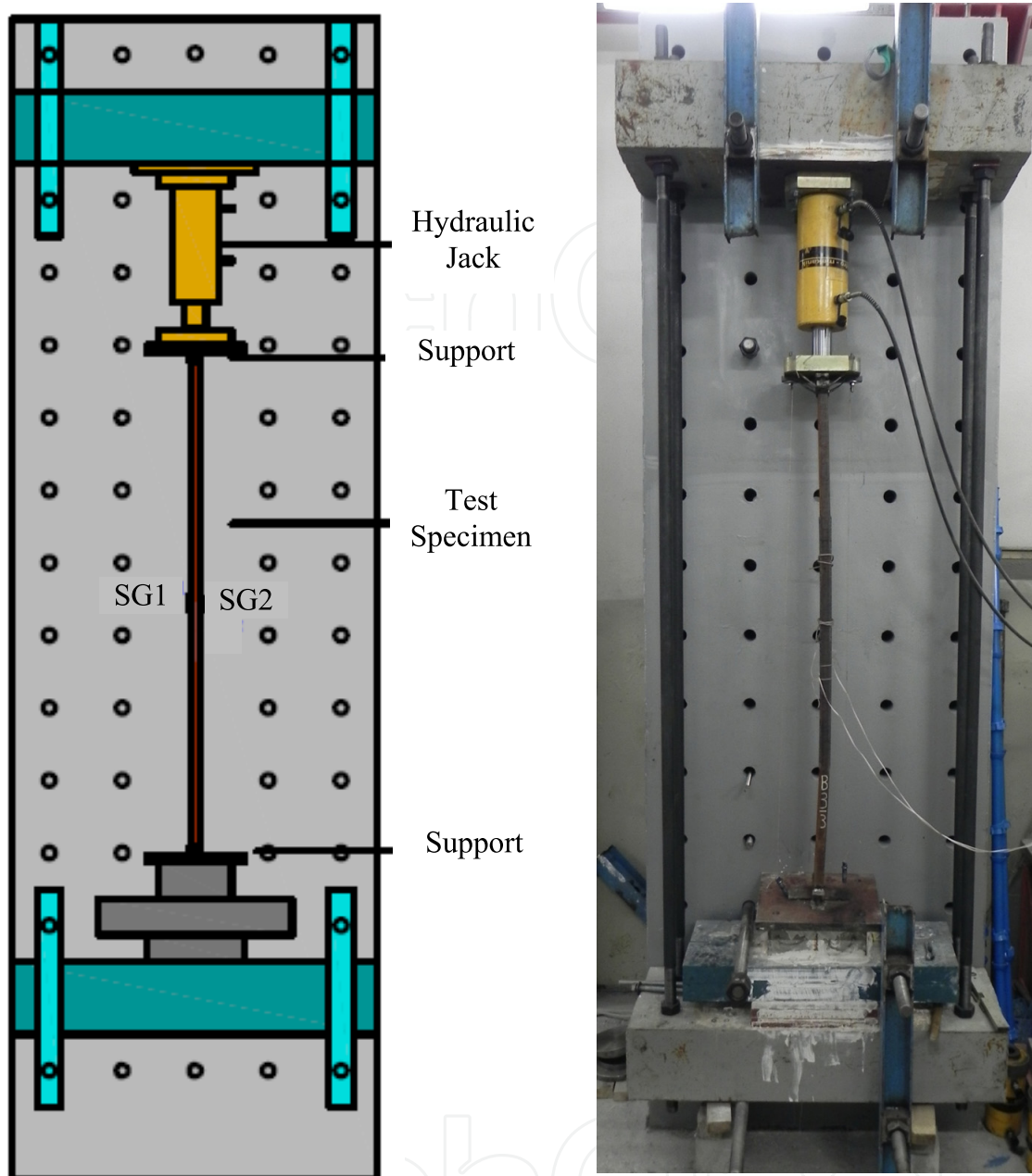


Figure 8. Test setup

As shown in Fig. 8, the test specimens are placed between the top and bottom supports in the test rig, which is rigidly connected to the strong reaction wall. To ensure minor-axis buckling of the test columns, the supports are designed in such a way that the rotation is about a single axis, resisting rotation about the orthogonal axis. In other words, the supports behave as pinned supports in minor-axis bending whereas fixed supports in major-axis bending. The compressive load is applied to the columns through a hydraulic jack placed at the top of the upper support. During the tests, in addition to the load readings, which are measured by a pressure gage, strains at the outermost fibers in the central cross section of each column are recorded via two strain gauges (SG1 and SG2) (see Fig. 8).

The buckled shapes of the tested columns are presented in Fig. 9 and Fig. 10. As shown in Fig. 9a, uniform columns buckle in the shape of a half-sine wave, which is in agreement with the well-known Euler's formulation for *ideal* pinned-pinned columns. In contrast to *ideal* columns, however, test columns have *not* buckled suddenly during the tests. This is mainly due to the fact that all test specimens have unavoidable initial crookedness. Even though the amount of these imperfections remain within the tolerances specified by the specifications, they cause bending of the specimens with the initiation of loading. This is also apparent from the graphs presented in Fig. 11. These graphs plot strain gage measurements taken at the opposite sides of the column faces (SG1 and SG2) during the test of each specimen with respect to the applied load values. The divergence of strain gage readings (SG1 and SG2) from each other as the load increases clearly indicates onset of the bending under axial compression. This is compatible with the expectations since as stated by Galambos (1998), "geometric imperfections, in the form of tolerable but unavoidable out-of-straightness of the column and/or eccentricity of the axial load, will introduce bending from the onset of loading". Even though the test columns start to bend at smaller load levels, they continue to carry additional loads until they reach their "buckling" capacities, which are characterized as the peak values of their load-strain curves.

The buckling loads of all test specimens are tabulated in Table 4. When the buckling loads of three uniform columns are compared, it is observed that the buckling load for Specimen B0-3 (150.18 kN) is larger than those for Specimens B0-1 (129.60 kN) and B0-2 (128.49 kN). When Fig. 11a is examined closely, it can be observed that strain gage measurements start to deviate from each other at larger loads in Specimen B0-3 than B-01 and B0-2. Thus, it can be concluded that the capacity difference among these specimens occurs *most probably* due to the fact that the initial out-of-straightness of Specimen B0-3 is much smaller than that of B-01 and B-02. When the load-strain plots of the stiffened specimens (Fig. 11b-d) are examined, similar trends are observed for specimens with larger load values in their own sets, e.g., B2-1 and B2-3 in the third set, B3-1 in the fourth set. These differences can also be attributed *partially* to the initial out-of-straightness. Unlike uniform columns, stiffened columns have additional initial imperfections due to the welding process of the stiffeners. It is now well known that welding cause unavoidable residual stresses to develop within the cross section of the member, which, in turn, can change the behavior of the member significantly. Since the columns with larger stiffened length ratios have longer welds, they are expected to have more initial imperfection. The effects of initial imperfections can also be seen from the last column of Table 4, where the ratios of experimental results to the analytical results which are obtained for *ideal* columns are presented.

For better comparison, experimental ($P_{cr,exp}$) and analytical ($P_{cr,analy}$) buckling loads are also plotted in Fig. 12. As shown in the figure, all test results lay below the analytical curve.

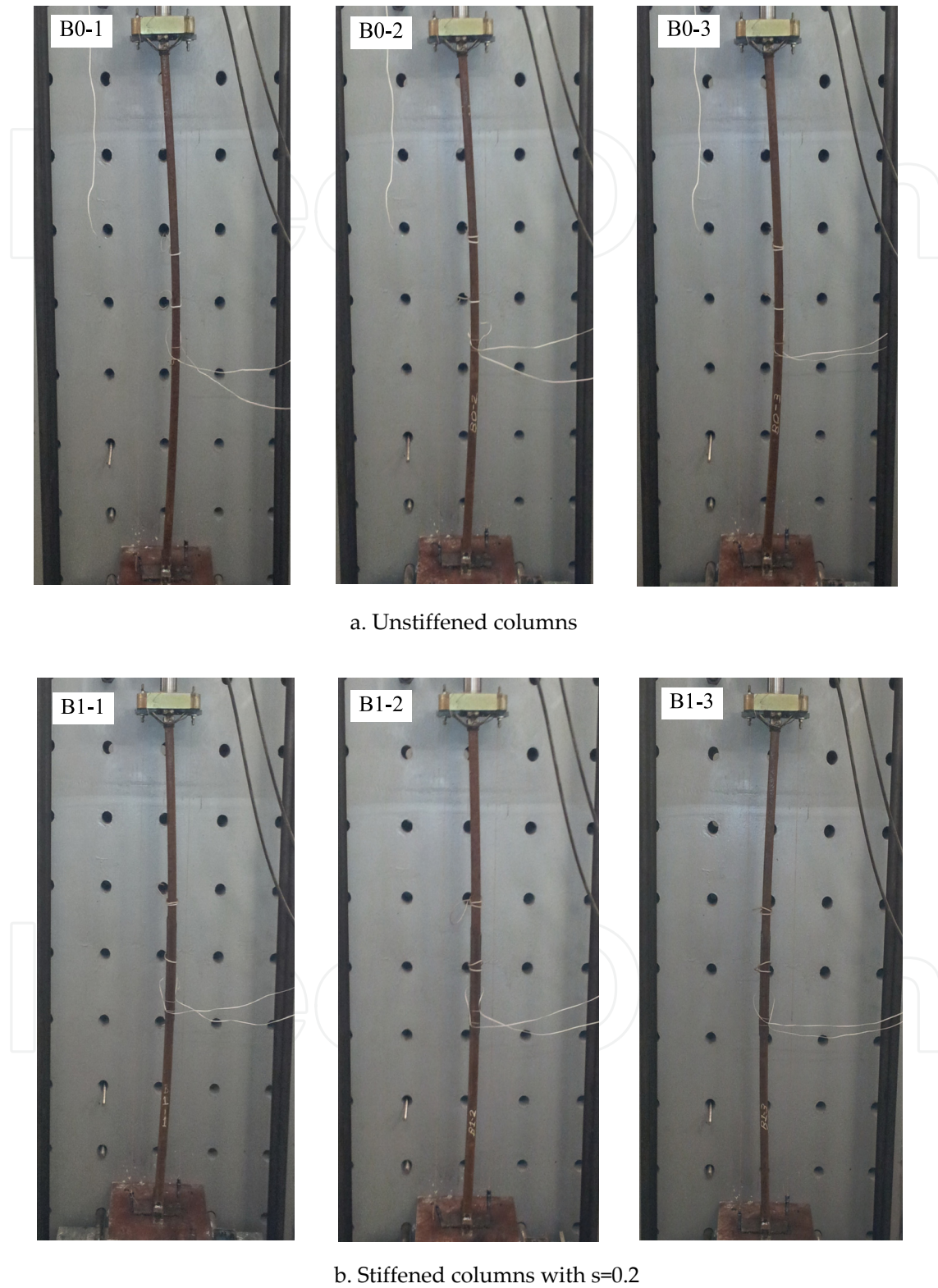
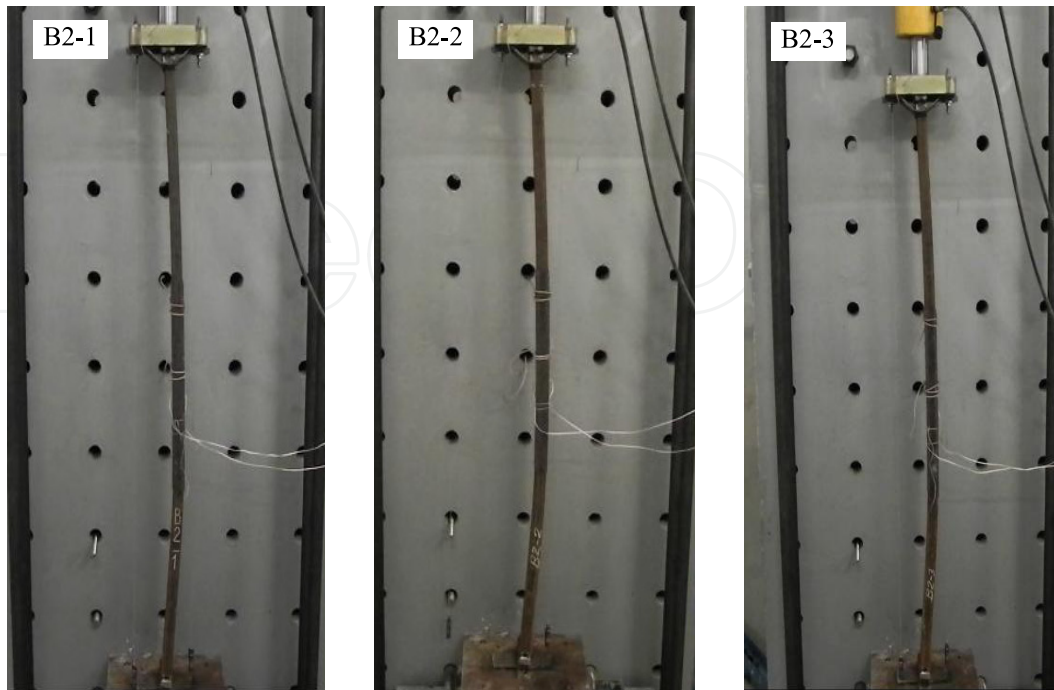
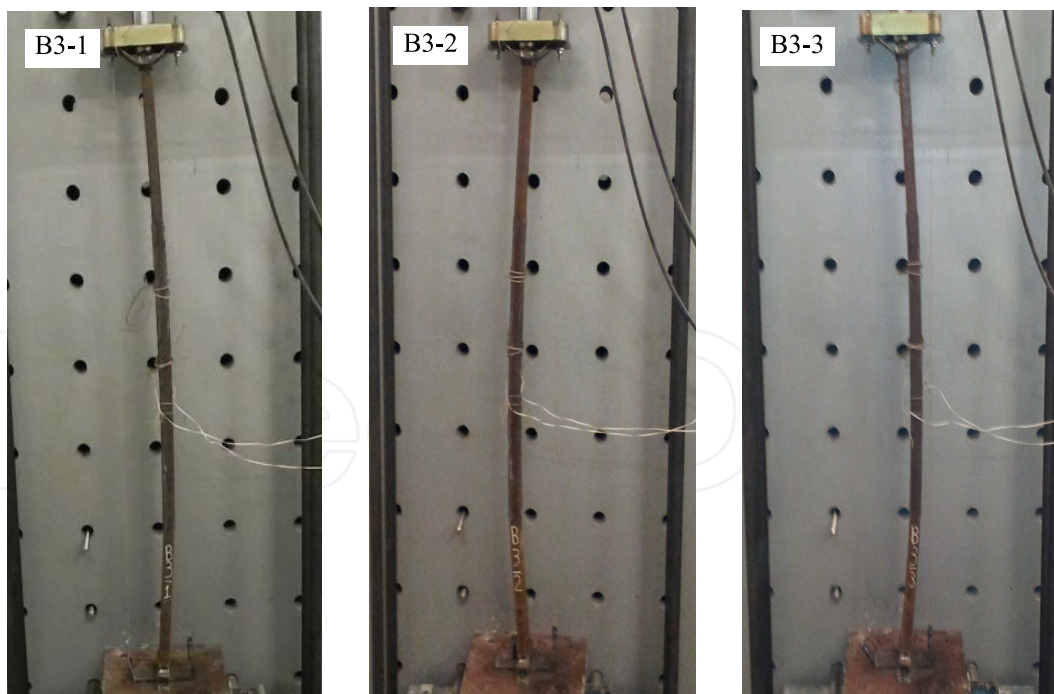


Figure 9. Buckled shapes of unstiffened and stiffened (with $s=0.2$) test specimens



a. Stiffened columns with $s=0.3333$



b. Stiffened columns with $s=0.5$

Figure 10. Buckled shapes of stiffened test specimens with $s=0.3333$ and $s=0.5$

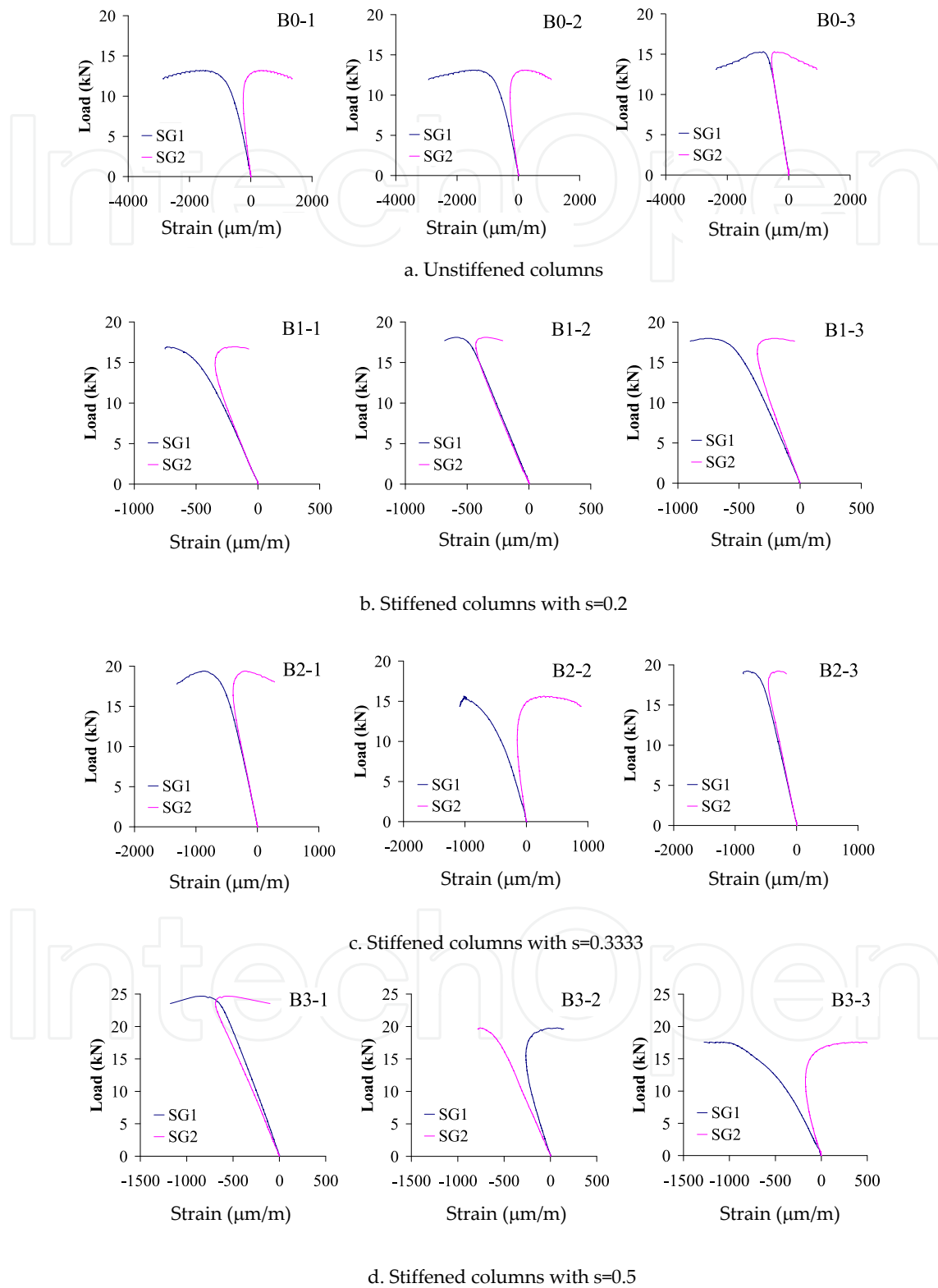


Figure 11. Load versus strain gage measurements for the test specimens

Specimen	s	$P_{cr,exp}$ (kN)	$P_{cr,analy}$ (kN)	$P_{cr,exp} / P_{cr,analy}$
B0-1	0	129.60	157.42	0.823
B0-2		128.49		0.816
B0-3		150.18		0.954
B1-1	0.2	166.31	192.98	0.862
B1-2		177.44		0.919
B1-3		176.32		0.914
B2-1	0.3333	190.23	221.78	0.858
B2-2		153.52		0.692
B2-3		188.56		0.850
B3-1	0.5	241.96	260.10	0.930
B3-2		194.12		0.746
B3-3		172.43		0.663

Table 4. Experimental buckling loads for uniform and stiffened columns compared with the analytical predictions

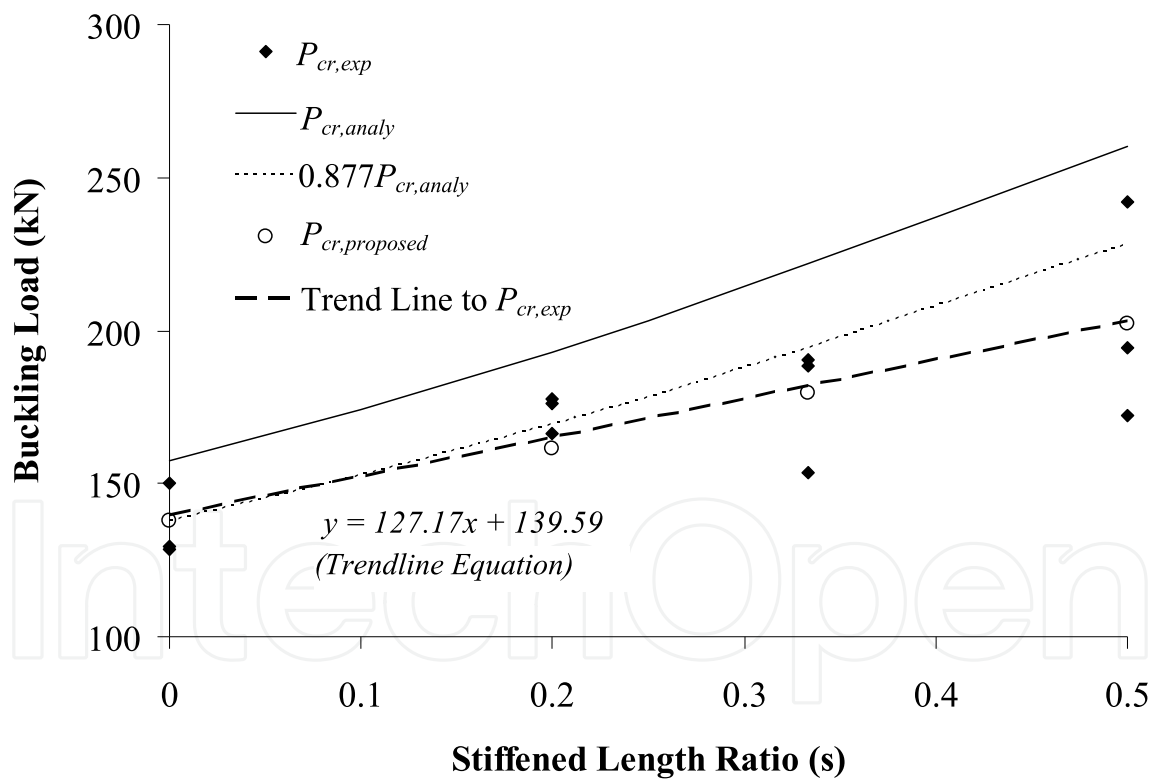


Figure 12. Experimental results compared with analytical and modified analytical buckling loads

It is important to note that most design specifications modify the buckling load equations derived for *ideal* columns to take into account the effects of initial out-of-straightness of the columns in the design of compression members. As an example, to reflect an initial out-of-straightness of about 1/1500, AISC (2010) modifies the “Euler” load by multiplying with a factor of 0.877 in the calculation of compressive capacity of elastically buckling members

(Salmon et al., 2009). By applying a similar modification to the analytical results obtained in this study for *ideal* three-segment compression members, a *more realistic* analytical curve is drawn. This curve is plotted in Fig. 12 with a label ' $0.877 P_{cr,analy}$ '. From Fig. 12, it is seen that the "modified" analytical curve *almost* "averages" most of the test results. The larger discrepancies observed in stiffened specimens with $s=0.3333$ and $s=0.5$ are believed to be resulted from the residual stresses locked in the specimens during welding of the steel stiffening plates, which highly depends on quality of workmanship. For this reason, while calculating the buckling load of a multi-segment compression member formed by welding, not only the initial out-of-straightness of the member, but also the effects of welding have to be taken into account. Considering that stiffened columns will always have more initial imperfections than uniform columns, it is suggested that a smaller modification factor be used in the design of multi-segment columns. Based on the limited test data obtained in the experimental phase of this study, the following modification factor is proposed to be used in the design of three-segment symmetric steel compression members formed by welding steel stiffening plates:

$$MF = (0.877 - 0.2s) \quad (25)$$

where s is the stiffened length ratio of the compression member, which equals to the weld length in the stiffened members. Thus, the proposed buckling load ($P_{cr,proposed}$) for such a member can be computed by modifying the analytical buckling load ($P_{cr,analy}$) as in the following expression:

$$P_{cr,proposed} = MF \times P_{cr,analy} \quad (26)$$

The proposed buckling loads for the multi-segment columns tested in the experimental part of this study are computed using Eq. (26) with Eq. (25) and plotted in Fig. 12 with a label ' $P_{cr,proposed}$ '. For easier comparison, a linear trend line fitted to the experimental data is also plotted in the same figure. Fig. 12 shows perfect match of design values of buckling loads with the trend line. While using Eq. (25), it should be kept in mind that the modification factor proposed in this paper is derived based on the limited test data obtained in the experimental part of this study and needs being verified by further studies.

5. Conclusion

In an attempt to design economic and aesthetic structures, many engineers nowadays prefer to use nonuniform members in their designs. Strengthening a steel braced structure which have insufficient lateral resistant by stiffening the braces through welding additional steel plates or wrapping fiber reinforced polymers in partial length is, for example, a special application of use of multi-segment nonuniform members in earthquake resistant structural engineering. The stability analysis of multi-segment (stepped) members is usually very complicated, however, due to the complex differential equations to be solved. In fact, most of the design formulae/charts given in design specifications are developed for uniform members. For this reason, there is a need for a practical tool to analyze buckling behavior of nonuniform members.

In this study, elastic buckling behavior of three-segment symmetric stepped compression members with pinned ends is analyzed using three different approaches: (i) analytical, (ii) numerical and (iii) experimental approaches. In the analytical study, first the governing equations of the studied stability problem are derived. Then, exact solution is obtained. Since exact solution requires finding the smallest root of a rather complex characteristic equation which highly depends on initial guess, the governing equations are also solved using a recently developed analytical technique, called Variational Iteration Method (VIM), and it is shown that it is much easier to solve the characteristic equation derived using VIM. The problem is also handled, for some special cases, by using widely known structural analysis program SAP2000 (CSI, 2008). Agreement of numerical results with analytical results indicates that such an analysis program can also be effectively used in stability analysis of stepped columns. Finally, aiming at the verification of the analytical results, the buckling loads of steel columns with hollow rectangular cross section stiffened, in partial length, by welding steel plates are investigated experimentally. Experimental results point out that the buckling loads obtained for *ideal* columns using analytical formulations have to be modified to reflect the initial imperfections. If welding is used while forming the stiffened members, as done in this study, not only the initial out-of-straightness, but also the effects of welding have to be considered in this modification. Based on the limited test data, a modification factor which is a linear function of the stiffened length ratio is proposed for three-segment symmetric steel compression members formed by welding steel plates in the stiffened regions.

Author details

Seval Pinarbasi Cuhadaroglu, Erkan Akpınar,
Fuad Okay, Hilal Meydanlı Atalay and Sevket Özden
Kocaeli University, Turkey

6. References

- Abulwafa, E.M.; Abdou, M.A. & Mahmoud, A.A. (2007). Nonlinear fluid flows in pipe-like domain problem using variational iteration method. *Chaos Solitons & Fractals*, Vol.32, No.4, pp. 1384–1397.
- American Institute of Steel Construction (AISC). (2010). *Specification for Structural Steel Buildings (AISC 360-10)*, Chicago.
- Atay, M.T. & Coskun, S.B. (2009). Elastic stability of Euler columns with a continuous elastic restraint using variational iteration method. *Computers and Mathematics with Applications*, Vol.58, pp. 2528-2534.
- Batiha, B.; Noorani, M.S.M. & Hashim, I. (2007). Application of variational iteration method to heat- and wave-like equations. *Physics Letters A*, Vol. 369, pp. 55-61.
- Computers and Structures Inc. (CSI) (2008) *SAP2000 Static and Dynamic Finite Element Analysis of Structures (Advanced 12.0.0)*, Berkeley, California.

- Coskun, S.B. & Atay, M.T. (2007). Analysis of convective straight and radial fins with temperature- dependent thermal conductivity using variational iteration method with comparison with respect to finite element analysis. *Mathematical Problems in Engineering*, Article ID: 42072.
- Coskun, S.B. & Atay, M.T. (2008). Fin efficiency analysis of convective straight fins with temperature dependent thermal conductivity using variational iteration method. *Applied Thermal Engineering*, Vol.28, No.17-18, pp. 2345-2352.
- Coskun, S.B. & Atay, M.T. (2009). Determination of critical buckling load for elastic columns of constant and variable cross-sections using variational iteration method. *Computers and Mathematics with Applications*, Vol.58, pp. 2260-2266.
- Ganji, D.D. & Sadighi, A. (2007). Application of homotopy-perturbation and variational iteration methods to nonlinear heat transfer and porous media equations. *Journal of Computational and Applied Mathematics*, Vol.207, pp. 24-34.
- Galambos, T.V. (1998). *Guide to Stability Design Criteria for Metal Structures* (fifth edition), John Wiley & Sons, Inc., ISBN 0-471-12742-6, New York.
- He, J.H. (1999). Variational iteration method - a kind of nonlinear analytical technique: some examples. *International Journal of Non Linear Mechanics*, Vol.34, No.4, pp. 699-708.
- He, J.H.; Wu, G.C. & Austin, F. (2010). The variational iteration method which should be followed. *Nonlinear Science Letters A*, Vol.1, No.1, pp. 1-30.
- Li, Q.S. (2001). Buckling of multi-step non-uniform beams with elastically restrained boundary conditions. *Journal of Constructional Steel Research*, Vol.57, pp. 753-777.
- Miansari, M.; Ganji, D.D. & Miansari M. (2008). Application of He's variational iteration method to nonlinear heat transfer equations. *Physics Letters A*, Vol. 372, pp. 779-785.
- Okay, F.; Atay, M.T. & Coskun S.B. (2010). Determination of buckling loads and mode shapes of a heavy vertical column under its own weight using the variational iteration method. *International Journal of Nonlinear Science Numerical Simulation*, Vol.11, No.10, pp. 851-857.
- Ozturk, B. (2009). Free vibration analysis of beam on elastic foundation by variational iteration method. *International Journal of Non Linear Mechanics*, Vol.10, No.10, pp. 1255-1262.
- Pinarbasi, S. (2011). Lateral torsional buckling of rectangular beams using variational iteration method. *Scientific Research and Essays*, Vol.6, No.6, pp. 1445-1457.
- Salmon, C.G.; Johnson, E.J. & Malhas, F.A. (2009). *Steel Structures, Design and Behavior* (fifth edition), Pearson, Prentice Hall, ISBN-10: 0-13-188556-1, New Jersey.
- Sweilam, N.H. & Khader, M.M. (2007). Variational iteration method for one dimensional nonlinear thermoelasticity. *Chaos Solitons & Fractals*, Vol.32, No.1, pp. 145-149.
- Timoshenko, S.P. & Gere, J.M. (1961). *Theory of Elastic Stability* (second edition), McGraw-Hill Book Company, ISBN- 0-07-085821-7, New York.